Atmos. Chem. Phys. Discuss., 3, 2331–2352, 2003
www.atmos-chem-phys.org/acpd/3/2331/

Atmospheric
Chemistry
and Physics
Discussions

Sensitivity studies of the recent new data on O(^1D) quantum yields in O_3 Hartley band photolysis in the stratosphere

N. Taniguchi[1], S. Hayashida[1], K. Takahashi[2], and Y. Matsumi[2]

[1]Faculty of Science, Nara Women's University, Kitauoya-Nishimachi, Nara, 630-8506, Japan
[2]Solar-Terrestrial Environment Laboratory, Nagoya University, Honohara 3–13, Toyokawa, 442-8507, Japan

Received: 3 February 2003 – Accepted: 14 April 2003 – Published: 12 May 2003

Correspondence to: N. Taniguchi (ntanig@ics.nara-wu.ac.jp)

Abstract

The production yields of excited oxygen O(^1D) atoms from the near ultraviolet O_3 photolysis are essential quantities for atmospheric chemistry calculations because of its importance as major sources of hydroxyl (OH) radicals and nitric oxide (NO). Recently, new O(^1D) quantum yields from O_3 photolysis between 230 and 305 nm in the Hartley band region were reported, which are almost independent of the photolysis wavelength (0.88–0.93) and smaller than NASA/JPL-2000 recommendation (0.95 between 240 and 300 nm). In order to assess consequences of the new data of O(^1D) quantum yields on the stratospheric chemistry, the changes in stratospheric chemical partitioning and O_3 concentration are examined using a one-dimensional atmospheric model. Our steady state model simulations for mid-latitude in March indicate that the smaller O(^1D) quantum yields result in increases of stratospheric O_3 (up to ~2% in the upper stratosphere), which are attributed to the changes in HO_x, NO_x, and ClO_x abundance and their catalyzed O_3 loss rates.

1. Introduction

Photodissociation by solar ultraviolet (UV) radiation drives much of the chemistry in the stratosphere and troposphere, since it contributes to the removal of many atmospheric trace gases by decomposition and generates highly reactive radicals. One of the important photochemical reactions is the photolysis of O_3 in the UV region, which produces O(^1D) atoms. Then, the produced O(^1D) radicals react with water vapor and generate OH radicals which rule the oxidation capacity of the atmosphere (Brasseur et al., 1999; Finlayson-Pitts and Pitts, 1999):

$$O_3 + h\upsilon \rightarrow O(^1D) + O_2(^1\Delta_g), \qquad (1)$$

$$\rightarrow O(^3P) + O_2(X^3\textstyle\sum_g^-), \qquad (2)$$

$$O(^1D) + H_2O \rightarrow 2OH. \quad (3)$$

The chemical reactions of $O(^1D)$ play important roles in determining the chemical composition of the stratosphere. Figure 1 illustrates the principal chemical reactions involving $O(^1D)$ in the stratosphere. Most of the $O(^1D)$ atoms produced by the photolysis of O_3 are quickly deactivated by collisions with major atmospheric species (M = N_2 and O_2) and then form O_3 molecules again:

$$O(^1D) + M \rightarrow O(^3P) + M, \quad (4)$$

$$O(^3P) + O_2 + M \rightarrow O_3 + M. \quad (5)$$

The production rate of stratospheric OH depends on the $O(^1D)$ production from O_3 photolysis. The OH radicals formed by reaction (3) initiate the HO_x catalytic cycle of O_3 loss, which is the main process for controlling O_3 loss in the lower and upper stratosphere. OH is directly involved in a HO_x catalytic cycle and also controls the partitioning between active species such as nitrogen oxides and chlorine oxides and their reservoirs:

$$OH + NO_2 + M \rightarrow HNO_3 + M, \quad (6)$$

$$OH + HCl \rightarrow Cl + H_2O. \quad (7)$$

The $O(^1D)$ also produces the NO radical in the stratosphere due to the reaction with N_2O:

$$O(^1D) + N_2O \rightarrow 2NO. \quad (8)$$

NO is the major catalyst for O_3 loss of NO_x in the middle stratosphere. NO_x also suppresses the halogen catalytic destruction of O_3 by sequestering them in unreactive forms such as $ClONO_2$:

$$NO_2 + ClO + M \rightarrow ClONO_2 + M. \quad (9)$$

The net effect on stratospheric O_3 depends on the relative contributions of these mechanisms at each altitude.

The channel branching ratios between channels (1) and (2) from O_3 photolysis have been examined extensively in the wavelength range $\lambda > 306$ nm at 298 K and low temperature by various laboratories over the past two decades (Matsumi et al., 2002, and references therein), which are used in the model calculation for such a comparison of observed and modeled OH, HO_x, and O_3 concentrations and photolysis rate of O_3 (e.g. Wennberg et al., 1999; Pfister et al., 2000). The $O(^1D)$ quantum yields in the photolysis of O_3 at wavelengths shorter than 300 nm have not received much attention and JPL-2000 evaluations for atmospheric modeling by NASA panel recommended the constant value of 0.95 for the wavelength range of 240–300 nm (Sander et al., 2000). The experimental data for the $O(^1D)$ quantum yields from O_3 photolysis over the Hartley band (200–300 nm) are sparse, which may result in some notable uncertainties in the model calculation. Very recently, Taniguchi et al. (2000) and Takahashi et al. (2002) have published results of the precise $O(^1D)$ quantum yield measurements in the photolysis of O_3 between 230 and 308 nm. The latest NASA/JPL panel (Sander et al. 2003) adopted the new experimental results of Taniguchi et al., they have recommend ~0.90 for $\lambda < 306$ nm. In this study, the atmospheric impacts of their laboratory results of $O(^1D)$ quantum yields from O_3 photolysis on the stratospheric chemistry have been explored, in the framework of a one-dimensional dynamical-photochemical model.

2. $O(^1D)$ quantum yield data in the photolysis of O_3

The absolute quantum yields of $O(^1D)$ formation from O_3 photolysis between 306 and 328 nm have been evaluated by the Matsumi et al. (2002) with the detailed examination of recent experimental measurements as a joint activity of SPARC and IGAC. Very recently, Takahashi et al. (2002) have measured the $O(^1D)$ quantum yields from O_3 photolysis between 230 and 308 nm using a new experimental technique. Using the same technique, Taniguchi et al. (2000) have indicated that the $O(^1D)$ quantum yield in the wavelength range of 297–306 nm is almost independent of the wavelength (~0.89). In Fig. 2, the yield values presented by Taniguchi et al. (2000) and Takahashi et al.

(2002) are compared with both values previously reported by other different groups (Trolier and Wiesenfeld, 1988; Cooper et al., 1993; Talukdar et al., 1997, 1998) and JPL-2000 recommendations (Sander et al., 2000). Talukdar et al. (1998) reported that the $O(^1D)$ quantum yield between 289 and 305 nm was 0.89 ± 0.02, which is in good agreement with results presented by Taniguchi et al. (2000) and Takahashi et al. (2002). The yield values reported by Trolier and Wiesenfeld (1988) and JPL-2000 recommendations in this wavelength region are larger than values reported by Talukdar et al. (1998) , Taniguchi et al. (2000), and Takahashi et al. (2002). At shorter wavelengths, JPL-2000 panel has recommended a constant value of 0.95 for the $O(^1D)$ quantum yield in the Hartley band photolysis of O_3 between 240 and 300 nm. The $O(^1D)$ quantum yields presented by Takahashi et al. (2002) are almost independent of the photolysis wavelengths (~0.91) between 230 and 300 nm, which are ~4–5% smaller than the JPL-2000 recommendation values and in good agreement with values determined by Cooper et al. (1993), except for 228.5 and 231 nm. Talukdar et al. (1997) reported the room temperature $O(^1D)$ quantum yield of 0.91 ± 0.06 at 248 nm, which is in good agreement with the value of 0.914 ± 0.019 presented by Takahashi et al. (2002). Talukdar et al. (1998) showed that the $O(^1D)$ quantum yields between 289 and 305 nm were independent of the temperature (203–320 K). Talukdar et al. (1997) and Takahashi et al. (1998) reported a negligible temperature dependence of $O(^1D)$ quantum yields at 248 nm and 305 nm, respectively. We have focused on the difference in the wavelength range of 230–305 nm between the new quantum yield values (Taniguchi et al., 2000; Takahashi et al., 2002) and JPL-2000 recommendations, and examined the consequences of the difference in the chemical compositions in the mid-latitude stratosphere using a one-dimensional chemical model. The effect of the difference of the $O(^1D)$ quantum yield values in the wavelength region of 230–305 nm should be significant in the stratosphere and very little in the troposphere, since the solar radiation at the wavelengths shorter than 305 nm mainly affects the stratospheric chemistry.

3. O(^1D) production rates in the stratosphere

The total production rates of O(^1D) atom from O_3 photolysis at several altitudes, $P_{\text{total}}(\text{O}^1D)$, were calculated by

$$P_{\text{total}}(\text{O}^1D) = \int P(\lambda)d\lambda = \int F(\lambda)\sigma(\lambda, T)\Phi_{1D}(\lambda, T)d\lambda, \tag{10}$$

where λ is the wavelength, and T is the temperature and F the actinic flux at the altitude. σ defines the absorption cross section of the O_3 molecule and Φ_{1D} the O(^1D) quantum yield from O_3 photolysis which is the probability for a process (1) to occur upon absorption of a photon. We calculated the $P_{\text{total}}(\text{O}^1D)$ values for the altitudes of 15, 25, and 40 km. The numerical data of F at solar zenith angle of 40° were taken from Finlayson-Pitts and Pitts (1999) and σ at 228 and 263 K were taken from Malicet et al. (1995) (Fig. 3). It should be noted that the relative O(^1D) production rate function, $P(\lambda)$, predominantly depends on the wavelength region ~230–320 nm, which is limited by the sunlight spectrum penetrating into the stratosphere and by the absorption properties of O_3 molecules. Therefore, the O(^1D) quantum yield from O_3 photolysis in this wavelength region and its temperature dependence is a key input parameter for modeling calculations in the stratospheric chemistry since the predominat source of the O(^1D) atoms in the stratosphere is the photolysis of O_3. Due to the temperature dependence of σ and Φ_{1D}, the ambient temperature influences the O(^1D) production rate functions at each altitude. At $\lambda > 310$ nm, the O(^1D) formation via photodissociation of the vibrationally and rotationally excited O_3 and spin-forbidden process takes place (Matsumi et al., 2002). Since the population of the internally excited O_3 molecules is dependent on the temperature, the O(^1D) quantum yields at $\lambda > 310$ nm (up to ~325 nm) change as a function of the temperature (Talukdar et al., 1998; Takahashi et al., 1998; Smith et al., 2000). In the calculations for the wavelengths longer than 308 nm, the expression for the O(^1D) quantum yields recommended by JPL-2000 (Sander et al., 2000) was used, which is a function of photolysis wavelength and temperature.

We found that the total O(^1D) production rates P_{total} (O^1D) estimated with the new O(^1D) quantum yields are smaller than those with the JPL-2000 recommendations by 2.5, 3.8 and 5.1%, at 15, 25 and 40 km, respectively. Atmospheric O_3 is photolyzed mainly by the UV radiation wavelength ~295–315 nm at 25 km and ~250–310 nm at 40 km, respectively. Therefore, the decreases in O(^1D) production rates caused by the new O(^1D) quantum yields in the wavelength range of 230–305 nm change the P_{total} (O^1D) more effectively at 40 km than that at 20 km. Comparisons of results obtained using the smaller values of O(^1D) quantum yields with those using the recommendations of JPL-2000 clearly suggest the significance of new O(^1D) yield data. Therefore, we examined the effects of the new O(^1D) yields on the stratospheric chemistry by model calculations, as described in the following section.

4. One-dimensional atmospheric model calculations

We have examined the effect of the smaller values of O(^1D) quantum yields (Taniguchi et al., 2000; Takahashi et al., 2002) using a one-dimensional dynamical-photochemical model, in which all the chemical reactions related to O_3 chemistry are reasonably represented and it is suitable for assessing the impact of the new O(^1D) quantum yield data on stratospheric chemistry. All chemical schemes in this one-dimensional model used here are the same as those used in the Garcia-Solomon two-dimensional (GS-2D) model (e.g. Solomon et al., 1996), which includes 90 kinetic reactions, 30 photolysis reactions, and 40 chemical species. Table 1 summarizes all 40 species included in this model. The model also includes actinic flux calculations. The reaction rate coefficients and absorption cross sections are updated to include NASA/JPL-1997 and -2000 recommendations (DeMore et al., 1997; Sander et al., 2000). Mixing ratios of 24 chemical species including O_3 for middle latitude in March are initialized, using data sets given by Brasseur et al. (1999) (Table 1). The vertical profiles of all species including the other photochemical species and families are computed to be in steady state for the day-night average condition. Since model responses of chemical species due to the change in $O(^1D)$ quantum yields represent the time-dependent propagation of infinitesimal perturbations, individual responses grow and converge on the time scale associated with that process. Therefore, calculations for all chemical species with the new values or JPL-2000 recommendations for the $O(^1D)$ quantum yields were run long enough to ensure convergence (±0.2% in concentration of all chemical species). The vertical profiles of O_3, HNO_3, and chemical families, HO_x, ClO_x, and NO_x, predicted by the model are illustrated in Fig. 4, when the new quantum yield values are used. Here, the families are defined as $HO_x = H + OH + HO_2$, $ClO_x = Cl + ClO$, and $NO_x = NO + NO_2$.

We have estimated how model concentration results for O_3 and other chemical species are affected when a new set of model parameters, that is, the new $O(^1D)$ quantum yields are adopted. The change in O_3 concentration, δO_3, is the relative change in a predicted model concentration:

$$\delta O_3 \equiv \frac{[O_3]_{\mathrm{New}} - [O_3]_{\mathrm{JPL}}}{[O_3]_{\mathrm{JPL}}}, \tag{11}$$

where $[O_3]_{\mathrm{New}}$ is concentration of O_3 calculated with the new values of $O(^1D)$ quantum yields from O_3 photolysis between 230 and 308 nm (Taniguchi et al., 2000; Takahashi et al., 2002), while $[O_3]_{\mathrm{JPL}}$ is that using JPL-2000 recommendations as a standard model (Sander et al., 2000). Figure 5 shows the results of the diurnally averaged photochemical model calculations, which indicates the change of the $O(^1D)$ and O_3 concentrations, $\delta O(^1D)$ and δO_3, versus altitude for latitudes of 20, 40, and 60° in March between the model runs with the new $O(^1D)$ values and the JPL-2000 recommendations. The partitioning changes in the chemical families, NO_x, HO_x, and ClO_x, predicted as a result of the parameter changes of $O(^1D)$ quantum yields from JPL-2000 recommendations to the new values are shown in Fig. 6.

Changes in the reactive families influence O_3 loss rates via the catalytic cycles involving those families. Figure 7 shows the O_3 loss rates by the three principal reactive families, NO_x, HO_x, and ClO_x, versus altitude for latitude of 40 degree in March, which were calculated based on the new $O(^1D)$ quantum yield values.

5. Discussions

The steady-state $O(^1D)$ concentration for latitude of 40° becomes smaller by ∼2–6% with a negative peak at 35 km due to the smaller $O(^1D)$ quantum yields from O_3 photolysis between 230 and 308 nm (Fig. 2), depending on altitude in the stratosphere as shown in Fig. 5. This result is consistent with our evaluation of the altitudinal changes in the total $O(^1D)$ production rate $P_{total}(O^1D)$. This indicates the consistency between the simple calculation with Eq. (10) and the one-dimensional chemical calculation, and that the concentration of $O(^1D)$ is influenced only by the production process of $O(^1D)$. The loss process of $O(^1D)$ is determined by the quenching process (4) which is not affected by the changes of the concentrations of minor species in the atmosphere. The O_3 concentration calculated with the new $O(^1D)$ quantum yields is higher than that with the JPL-2000 recommendations throughout the stratosphere. It should be noted that the change in the $O(^1D)$ concentration influences O_3 abundance even though atmospheric concentration of $O(^1D)$ atoms is much lower than O_3 concentration, since the $O(^1D)$ reactions (3) and (8) are the direct source for stratospheric HO_x and NO_x molecules which control the stratospheric radical partitioning and O_3 abundance through catalytic reactions (Fig. 1). The calculated response of O_3 concentration from these changes in the concentration of HO_x and NO_x is different between the upper, middle, and lower stratospheres because of the interdependence of the O_3 loss catalytic cycles.

As shown in Figs. 5 and 6, the absolute change in the stratospheric O_3 concentration is the largest at ∼40–45 km (increase up to ∼2%). This results from effect of the suppression of O_3 loss by the decrease of the NO_x, HO_x, and ClO_x concentrations in their catalytic O_3 loss cycles (Fig. 6). Figure 7 shows that total O_3 loss rate, that is, the sum of the O_3 loss rates in NO_x, HO_x, and ClO_x catalytic cycles has a peak around 40 km. Changes in O_3 loss rates in NO_x, HO_x, and ClO_x catalytic cycles, which were calculated from model runs with the new O(^1D) quantum yields and with the JPL-2000 recommendations, were similar to changes in NO_x, HO_x, and ClO_x concentrations which are shown in Fig. 6. Above this region, the contribution of the HO_x cycle becomes predominant drastically as the altitude increases (Fig. 7). The HO_x concentration in the upper stratosphere is decreased by the decrease of the OH formation trough reaction (3) due to the smaller O(^1D) quantum yield (Fig. 6). In the upper stratosphere, atomic O(^3P) constitutes efficiently the following catalytic cycle in which the rate-limiting step in the cycle is reaction (12):

$$OH + O_3 \rightarrow HO_2 + O_2, \tag{12}$$

$$HO_2 + O \rightarrow OH + O_2, \tag{13}$$

$$(\text{Net}: O + O_3 \rightarrow 2O_2).$$

Therefore, the decrease in HO_x concentration in the upper stratosphere caused by the smaller O(^1D) quantum yields results in the O_3 concentration increase most effectively in this region. On the other hand, HO_x concentration increases in the middle and lower stratosphere (Fig. 6). The NO_x concentration is reduced by the decrease of the O(^1D) formation via reaction (8). This reduction of the NO_x concentration takes place throughout the stratosphere. The increase of HO_x concentration in the middle and lower stratosphere may be attributed to the decrease of the rate of reaction (6) due to the smaller concentration of NO_x. Since the contribution of three-body reaction (6) becomes more significant at lower stratospheric altitudes, HO_x increases in the lower stratosphere as shown in Fig. 6.

ClO_x concentration also decreases in the upper-middle stratosphere with the smaller O(^1D) quantum yields, and a little increases in the lower stratosphere. The behavior of ClO_x concentration change is similar to that of HO_x concentration. The chlorine reservoir compound HCl is probably activated to ClO_x by reaction (7), that is, the reaction between OH and HCl (Fig. 1). The decreased OH production rate due to the smaller O(^1D) quantum yield results in the smaller ClO_x concentration. In the lower stratosphere, the decrease of the third body reaction (9) with smaller NO_x concentration may lead to the increase of ClO_x. ClO_x cycle is important especially around 45 km and accounts for about ~35% of the total O_3 loss rate in this region (Fig. 7).

As shown in Fig. 6, NO_x concentration is decreased throughout the stratosphere by the smaller $O(^1D)$ quantum yields, while the enhancement of O_3 takes place around 20–25 km (up to ~1%), but slightly less around 30 km. In the middle stratosphere, the NO_x catalytic cycle has the largest effect on the O_3 reduction (Fig. 7). The enhancements of O_3 concentration around 20–25 km with the new $O(^1D)$ quantum yields should be attributed to the decrease of NO_x catalytic O_3 loss.

In the upper stratosphere and mesosphere, a number of models cause an underprediction of O_3 concentrations at 40–50 km altitude compared to observations, with magnitude of the discrepancy increasing with altitude (Eluszkiewicz and Allen, 1993). This has been known as the "ozone deficit" problem. In the upper stratosphere, the chemical composition is determined by chemical processes that are faster than the relevant dynamical processes. Crutzen et al. (1995) and Grooß et al. (1999) have investigated the O_3 budget in the upper stratosphere in comparison with observations and photochemical modeling. They have pointed out that the uncertainty in the model parameters is a large source of the discrepancy although improvement of the observation quality and updated the latest model parameters decreases a significant ozone deficit. Smith et al. (2001) estimated O_3 uncertainties near 12% modeled in the middle and upper stratosphere, increasing in the lower stratosphere, from the JPL-2000 recommendations which significantly reduced several key reaction uncertainty values by laboratory measurements, that is, total catalytic photochemical uncertainty in model O_3 compared with a previous modeling. The enhancement of O_3 concentration in our chemical model calculations around 40–50 km altitude may contribute to precise assessment of the photochemical O_3 budget including the "ozone deficit" problem.

Title Page
Abstract | Introduction
Conclusions | References
Tables | Figures
◀| |▶
◀ ▶
Back | Close
Full Screen / Esc
Print Version
Interactive Discussion

6. Conclusions

Consequences of the new data of O(^1D) quantum yields from O_3 photolysis between 230 and 305 nm in the Hartley band region on the stratospheric chemistry are examined using a one-dimensional atmospheric model. Our sensitivity studies for mid-latitude in March indicate that the smaller O(^1D) quantum yields increase the O_3 concentration throughout stratosphere via a decrease in the importance of NO_x concentration in the middle stratosphere and the HO_x in the upper stratosphere.

Acknowledgement. N. T. thanks the Japan Society for Promotion of Science for a fellowship for young scientists. The one-dimensional model used in this study was originally offered by S. Solomon, NOAA Aeronomy Laboratory. N. T. gives special thank to M. Kawasaki, Kyoto University, for his helpful discussions and encouragements. This work was partly supported by a Grant-in-Aid from the Ministry of Education, Culture, Sports, Science and Technology, Japan.

References

Brassuer, G. P., Orlando, J. J., and Tyndall, G. S.: Atmospheric Chemistry and Global Change, Oxford University Press, 1999.

Cooper, I. A., Neill, P. J., and Wiesenfeld, J. R.: Relative quantum yield of O($^1D_2$) following ozone photolysis between 221 and 243.5 nm, J. Geophys. Res., 98, 12 795–12 800, 1993.

Crutzen, P. J., Grooß, J.-U., Brühl, C., Müller, R., and Russell III, J. M.: A Reevaluation of the Ozone Budget with HALOE UARS Data: No Evidence for the Ozone Deficit, Science, 268, 705–708, 1995.

DeMore, W. P., Sander, S. P., Howard, C. J., Ravishankara, A. R., Golden, D. M., Kolb, C. E., Hampson, R. F., Kurylo, M. J., and Molina, M. J.: Chemical Kinetics and Photochemical Data for Use in Stratospheric Modeling, JPL Publication 97-4, JPL, Pasadena, CA, 1997.

Eluszkiewicz, J. and Allen, M.: A global analysis of the ozone deficit in the upper stratosphere and lower mesosphere, J. Geophys. Res., 98, 1069–1082, 1993.

Finlayson-Pitts, B. J. and Pitts Jr., J. N.: Chemistry of the Upper and Lower Atmosphere: Theory, Experiments, and Applications, Academic Press, San Diego, 1999.

Grooß, J.-U., Müller, R., Becker, G., Mckenna, D. S., and Crutzen, P. J.: The upper stratospheric ozone budget: An update of calculations based on HALOE data, J. Atmos. Chem., 34, 171–183, 1999.

Malicet, J., Daumont, D., Charbonnier, J., Parisse, C., Chakir, A., and Brion, J.: Ozone UV spectroscopy. II. Absorption cross-sections and temperature dependence, J. Atmos. Chem., 21, 263–273, 1995.

Matsumi, Y., Comes, F.J., Hancock, G., Hofzumahaus, A., Hynes, A. J., Kawasaki, M., and Ravishankara, A. R.: Quantum yields for production of O(^{1}D) in the ultraviolet photolysis of ozone: Recommendation based on evaluation of laboratory data, J. Geophys. Res., 107, D3, 4024, doi:10.1029/2001JD000510, 2002.

Pfister, G., Baumgartner, D., Maderbacher, R., and Putz, E.: Aircraft measurements of photolysis rate coefficients for ozone and nitrogen dioxide under cloudy conditions, Atmos. Environ., 34, 4019–4029, 2000.

Sander, S. P., Friedl, R. R., DeMore, W. B., Golden, D. M., Kurylo, M. J., Hampson, R. F., Huie, R. E., Moortgat, G. K., Ravishankara, A. R., Kolb, C. E., Molina, M. J.: Chemical Kinetics and Photochemical Data for use in Stratospheric Modeling, JPL Publication 00-3, Evaluation Number 13, Jet Propulsion Laboratory, Pasadena, CA, 2000.

Sander, S. P., Friedl, R. R., Golden, D. M., Kurylo, M. J., Huie, R. E., Orkin, V. L., Moortgat, G. K., Ravishankara, A. R., Kolb, C. E., and Molina, M. J.: Chemical Kinetics and Photochemical Data for use in Atmospheric Studies, JPL Publication 02-25, Evaluation Number 14, Jet Propulsion Laboratory, Pasadena, CA, 2003.

Smith, G. D., Molina, L. T., and Molina, M. J.: Temperature Dependence of O(^{1}D) Quantum Yields from the Photolysis of Ozone between 295 and 338 nm, J. Phys. Chem., A 104, 8916–8921, 2000.

Smith, G. P., Dubey, M. K., Kinnison, D. E., and Connell, P. S.: Assessing Effects of Rate Parameter Changes on Ozone Models Using Sensitivity Analysis, J. Phys. Chem., A 105, 1449–1455, 2001.

Solomon, S., Portmann, R. W., Garcia, R. R., Thomason, L. W., Poole, L. R., and McCormick, M. P.: The role of aerosol variations in anthropogenic ozone depletion at northern midlatitudes, J. Geophys. Res., 101, 6713–6727, 1996.

Takahashi, K., Taniguchi, N., Matsumi, Y., Kawasaki, M., and Ashfold, M. N. R.: Wavelength and temperature dependence of the absolute O(^{1}D) production yield from the 305–329 nm photodissociation of ozone, J. Chem. Phys., 108, 7161–7172, 1998.

Takahashi, K., Hayashi, S., Matsumi, Y., Taniguchi, N., and Hayashida, S.: Quantum yields of O(^1D) formation in the photolysis of ozone between 230 and 308 nm, J. Geophys. Res., 107(D20), 4440, doi:10.1029/2001JD002048, 2002.

Talukdar, R. K., Gilles, M. K., Battin-Leclerc, F., Ravishankara, A. R., Fracheboud, J.-M., Orlando, J. J., and Tyndall, G. S.: Photolysis of ozone at 308 and 248 nm: Quantum yield of O(^1D) as a function of temperature, Geophys. Res. Lett., 24, 1091–1094, 1997.

Talukdar, R. K., Langfellow, C. A., Gilles, M. K., and Ravishankara, A. R.: Quantum yields of O(^1D) in the photolysis of ozone between 289 and 329 nm as a function of temperature, Geophys. Res. Lett., 25, 143–146, 1998.

Taniguchi, N., Takahashi, K., and Matsumi, Y.: Photodissociation of O_3 around 309 nm, J. Phys. Chem., A 104, 8936–8944, 2000.

Trolier, M. and Wiesenfeld, J. R.: Relative quantum yield of O($^1D_2$) following ozone photolysis between 275 and 325 nm, J. Geophys. Res., 93, 7119–7124, 1988.

Wennberg, P. O., Salawitch, R. J., Donaldson, D. J., Hanisco, T. F., Lanzendorf, E. J., Perkins, K. K., Lloyd, S. A., Vaida, V., Gao, R. S., Hintsa, E. J., Cohen, R. C., Swaetz, W. H., Kusterer, T. L., and Anderson, D. E.: Twilight observations suggest unknown sources of HO_x, Geophys. Res. Lett., 26, 1373–1376, 1999.

Table 1. List of chemical species used in the one-dimensional dynamical-photochemical model calculations

Initially set by Brasseur et al. (1999)					
O_3	H	OH	HO_2	H_2O_2	N
NO	NO_2	N_2O_5	HNO_4	HNO_3	H_2O
CH_4	N_2O	Cl	ClO	HOCl	$ClONO_2$
HCl	CCl_4	$CFCl_3$	CF_2Cl_2	CH_3Cl	CO
Calculated to be in steady state					
O(^3P)	O(^1D)	NO_3	Cl_2	Cl_2O_2	OClO
HBr	Br	BrO	HOBr	$BrONO_2$	CO_2
H_2	ClOO	$CHClF_2$	CH_3Br		

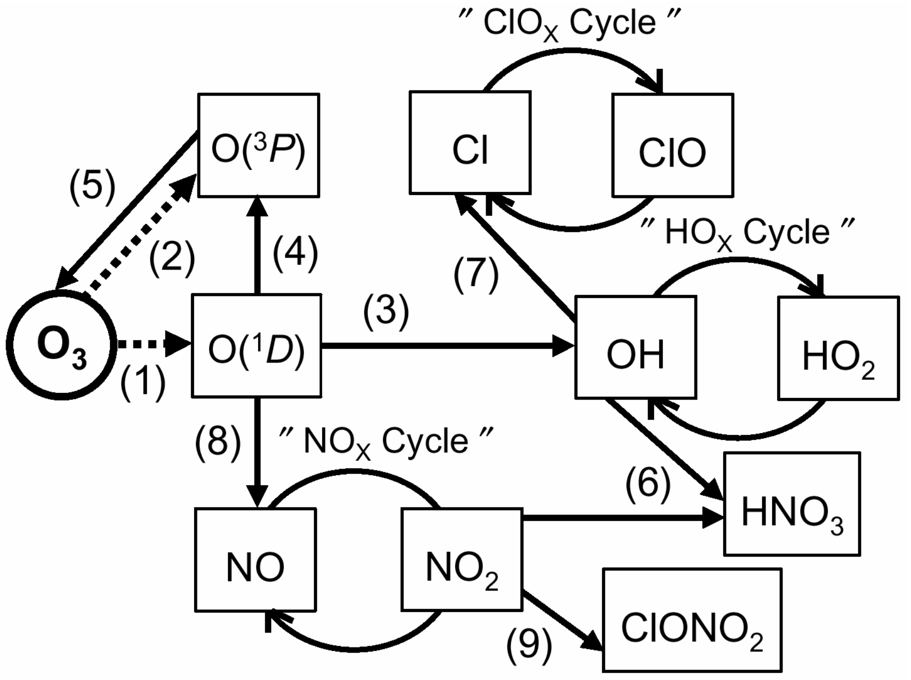

Fig. 1. Schematic of the reaction pathways involving O(^1D) formation in the O_3 photolysis in the stratosphere. Dash line means a photolysis reaction. Numbers given in parentheses correspond to reaction numbers shown in the text.

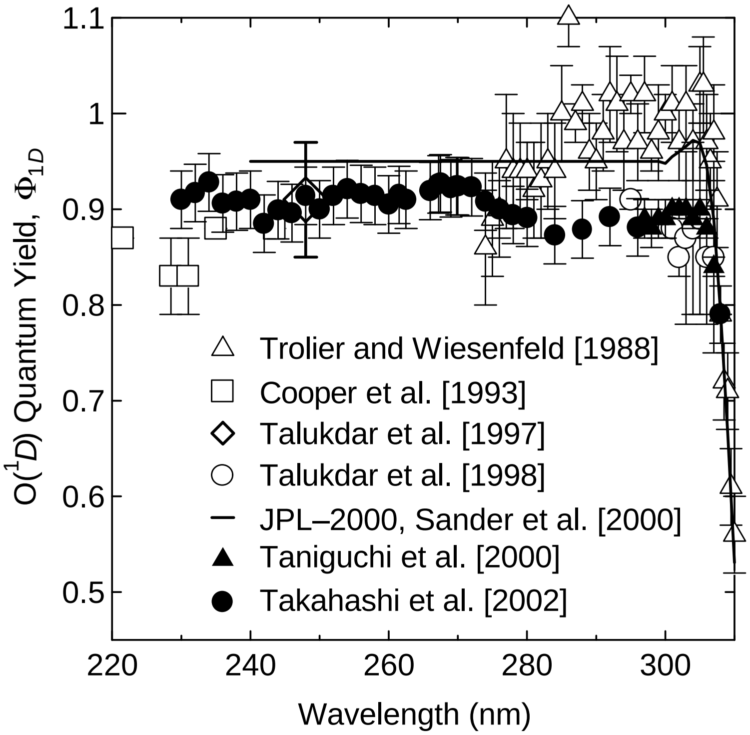

Fig. 2. The quantum yields for O(^1D) formation in the Hartley band photolysis of O_3 obtained by Taniguchi et al. (2000) and Takahashi et al. (2002). For comparison, the yield values reported by other groups are also shown (Trolier and Wiesenfeld, 1988; Cooper et al., 1993; Talukdar et al., 1997, 1998). Solid line indicates the yield values recommended by JPL-2000 evaluations for atmospheric modeling by NASA panel (Sander et al., 2000), which are constant (0.95) between 240 and 300 nm.

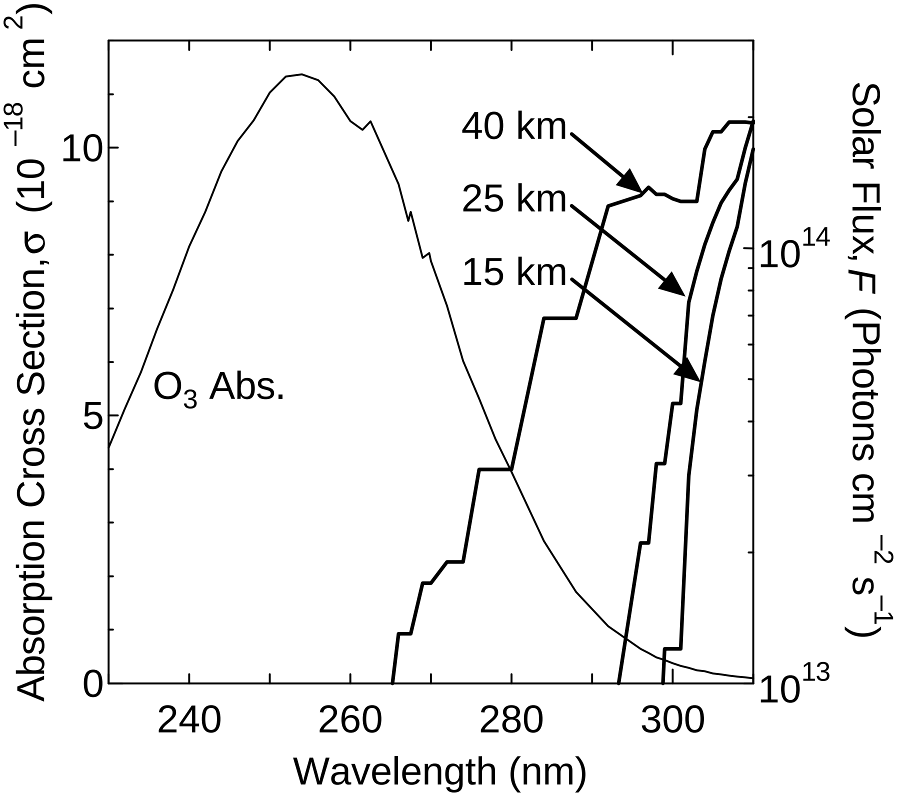

Fig. 3. Ultraviolet absorption spectrum of O_3 in the Hartley band at 263 K (Malicet et al., 1995) and actinic fluxes as a function of altitudes of 15, 25, and 40 km when the solar zenith angle is 40° (Finlayson-Pitts and Pitts, 1999).

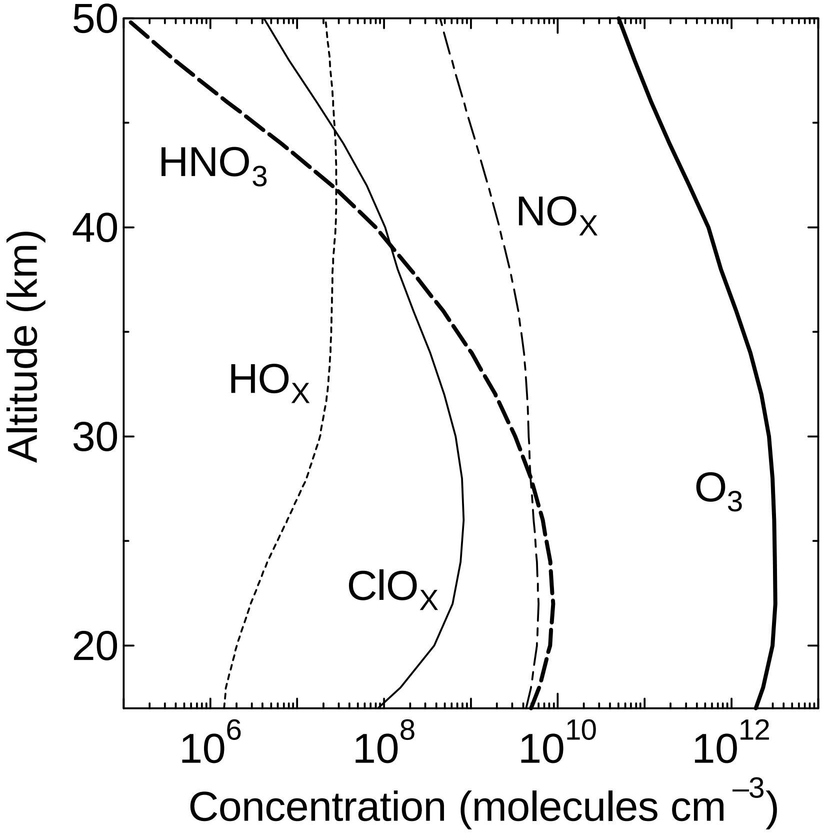

Fig. 4. Results of the one-dimensional chemical model calculations. Diurnally averaged vertical profiles of NO_x, HO_x, ClO_x, HNO_3 and O_3 (dot-dash, dot, solid, thick dash, and thick solid lines, respectively) predicted for latitude of 40° in March using the $O(^1D)$ quantum yield values measured by Taniguchi et al. (2000) and Takahashi et al. (2002).

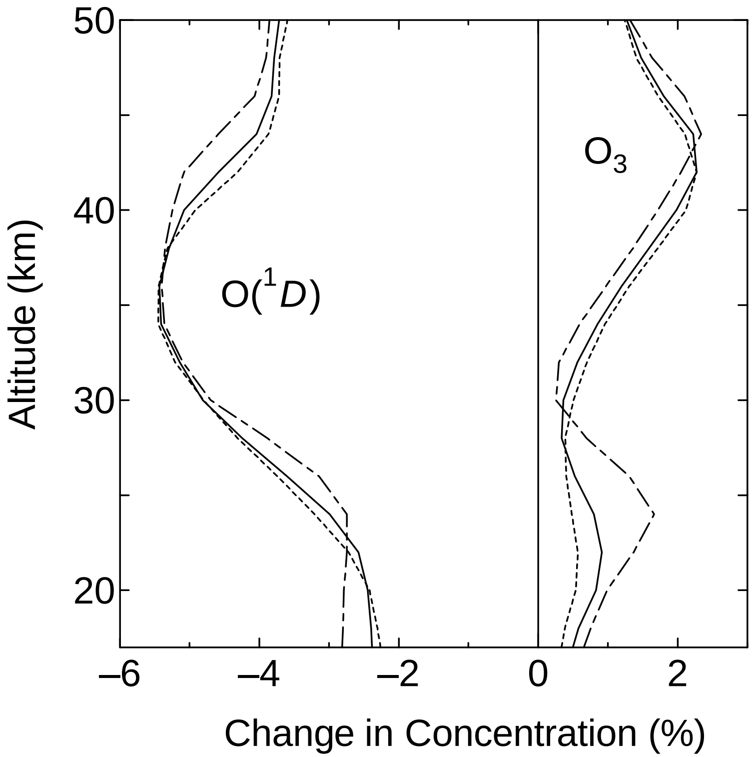

Fig. 5. Results of the one-dimensional chemical model calculations. The percentage changes in diurnally averaged $O(^1D)$ and O_3 concentrations predicted for latitude of 20, 40, and 60° (dot, solid, and dot-dash lines, respectively) in March as a function of altitude using the $O(^1D)$ quantum yield values measured by Taniguchi et al. (2000) and Takahashi et al. (2002), relative to those predicted using JPL-2000 recommendations for atmospheric modeling by NASA evaluation panel (Sander et al., 2000), that is, $\delta O(^1D)$ and δO_3 defined by Eq. (11) in the text.

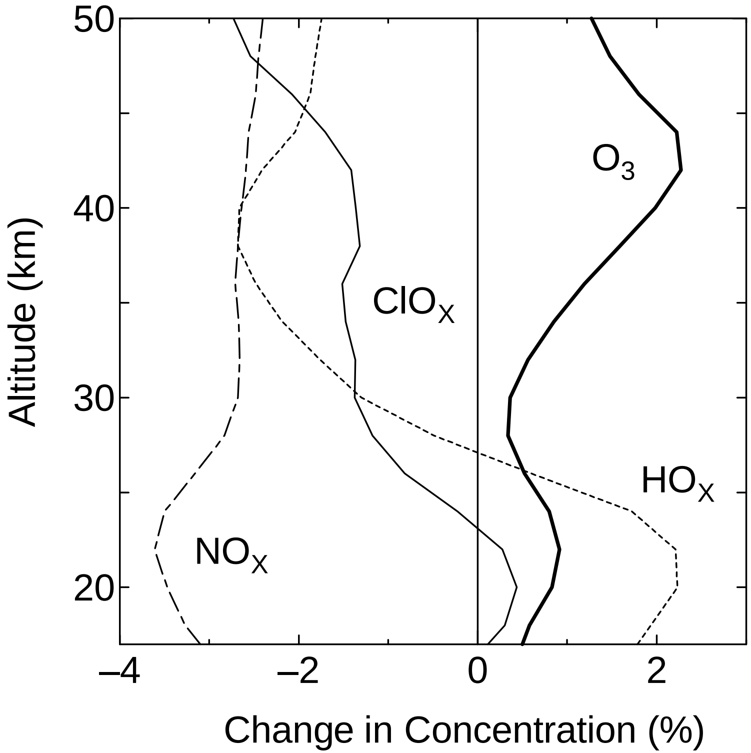

Fig. 6. Results of the one-dimensional chemical model calculations. The percentage changes in durnally averaged NO_x, HO_x, ClO_x, and O_3 concentrations (dot-dash, dot, solid, and thick lines, respectively) predicted for latitude of 40° in March as a function of altitude using the $O(^1D)$ quantum yield values measured by Taniguchi et al. (2000) and Takahashi et al. (2002), relative to those predicted using JPL-2000 recommendations for atmospheric modeling by NASA evaluation panel (Sander et al., 2000).

Title Page
Abstract | Introduction
Conclusions | References
Tables | Figures
◀◀ | ▶▶
◀ | ▶
Back | Close
Full Screen / Esc
Print Version
Interactive Discussion

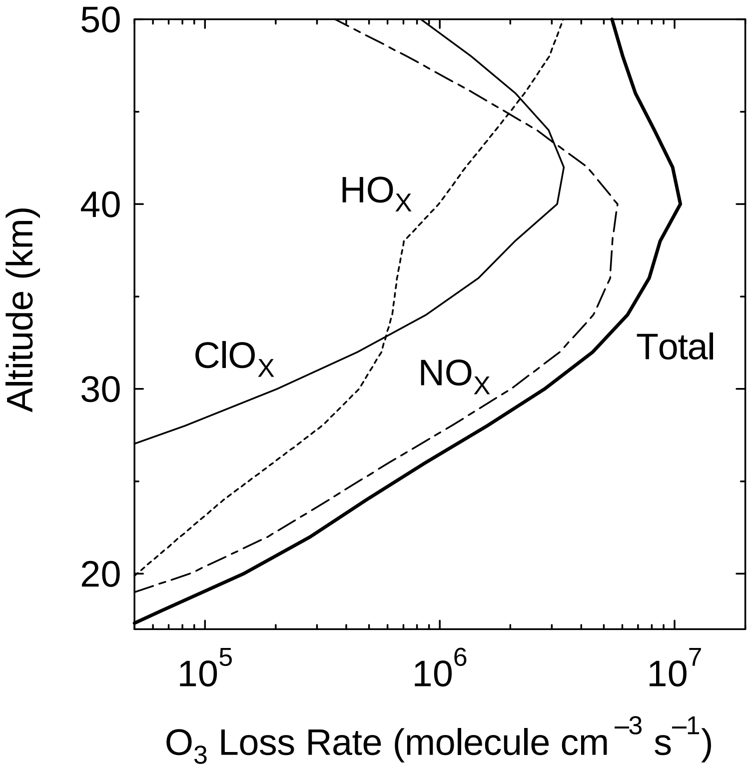

Fig. 7. Results of the one-dimensional chemical model calculations. Diurnally averaged O_3 loss rates due to NO_x, HO_x, and ClO_x chemistry (dot-dash, dot, and solid lines, respectively) predicted for latitude of 40° in March using the $O(^1D)$ quantum yield values measured by Taniguchi et al. (2000) and Takahashi et al. (2002). Thick line shows the total O_3 loss rate which is the sum of the O_3 loss rates in NO_x, HO_x, and ClO_x catalytic cycles.